Journal of Applied Polymer Science

Assembly and antibacterial activity of horizontally oriented silver nanoplates

Renjie Zhang,[1,2,3] Yongqing Kang,[2] Beibei Xie[2]

[1]National Engineering Technology Research Center for Colloidal Materials, Shandong University, Jinan 250199, People's Republic of China

[2]Key Laboratory of Colloid and Interface Chemistry of the Ministry of Education, Shandong University, Jinan 250199, People's Republic of China

[3]Key Laboratory of Special Functional Aggregated Materials of the Ministry of Education, Shandong University, Jinan 250199, People's Republic of China

Correspondence to: R. Zhang (E-mail: zhrj@sdu.edu.cn)

ABSTRACT: This work describes a strategy of assembling horizontally oriented Ag nanoplates (AgNPTs) with PSS-Ag as the precursor of silver by the layer-by-layer (LbL) technique on planar substrates. These AgNPTs have a lateral dimension of 20–80 nm and a thickness of 9–12 nm. A corresponding formation mechanism of these AgNPTs is discussed considering the orientation of the polyelectrolytes molecules, as well as their confinement effect on the diffusion of Ag nanoparticles. The exposed horizontal surfaces of the AgNPTs correspond to low free energy; they show an active antimicrobial activity. No *Staphylococcus aureus* colonies appear on the nutrient agar medium inoculated and incubated with *S. aureus* solutions treated by LbL films containing AgNPTs. The horizontally oriented AgNPTs by the described strategy in this work not only provides a novel method for controlled assembly of AgNPTs, but also provides insight in the antimicrobial behavior of nanoplate surfaces with low free energy. © 2015 Wiley Periodicals, Inc. J. Appl. Polym. Sci. **2015**, *132*, 42070.

KEYWORDS: biomaterials; nanoparticles; nanowires and nanocrystals; polyelectrolytes; self-assembly; surfaces and interfaces

Received 20 February 2014; accepted 30 January 2015

DOI: 10.1002/app.42070

INTRODUCTION

Synthesis of Ag nanoplates (AgNPTs)[1–4] will benefit optical biosensor,[5] cell performance and photo-current density with enhanced power conversion efficiency,[6] catalyst,[7] surface-enhanced resonance scattering (SERS) substrate,[8] and antibacterial activities.[9–11] However, in many synthesis either organic solvents like *N*,*N*-dimethylformamide[12] or solvothermal processes involving organic solvents, high temperature, and long reaction time[3,13,14] are needed. These synthesis of AgNPTs are either environmental unfriendly or energy consuming. In addition, there is a challenge of controlled assembly for AgNPTs, whose properties including the UV–vis spectra are novel.[15] So far only vertically oriented AgNPTs on solid substrates have been reported by an electrochemical method.[16,17] There are few articles on assembly of horizontally oriented AgNPTs.

The promising layer-by-layer (LbL) technique enables the layered structure of polyelectrolytes,[18] which can orient the Ag^+ cations in the polyelectrolyte-Ag complexes. A potential formation strategy of AgNPTs might be the reduction of such oriented Ag on planar solid substrates, which is also an extensive study on the LbL technique for applied interfaces and materials. This work confirms this novel strategy and horizontally oriented AgNPTs are assembled. The LbL without organic solvents is environmental friendly; and the assembly process is at room temperature. So this synthesis strategy of AgNPTs is superior to the above literature ones.

Regarding to the free energy of surfaces, crystal faces with high energies grow quickly, while observed crystal faces in large proportions correspond to low free energies.[19–21] Do such exposed surfaces of low free energies in AgNPTs show active antimicrobial activity? Confirmed answer to this question is given in this work by studying the *Staphylococcus aureus* (*S. aureus*) colonies on the nutrient agar medium inoculated and incubated with *S. aureus* solutions treated by LbL films containing the AgNPTs.

EXPERIMENTAL

Materials

The sources of reagents and materials were as follows: poly(sodium 4-styrenesulfonate) (PSS, M.W. ~70,000), poly(allylamine hydrochloride) (PAH, M.W. ~70,000) and *S. aureus* lyophilized pellet were obtained from Sigma-Aldrich Inc. HCl, H_2SO_4, 30%

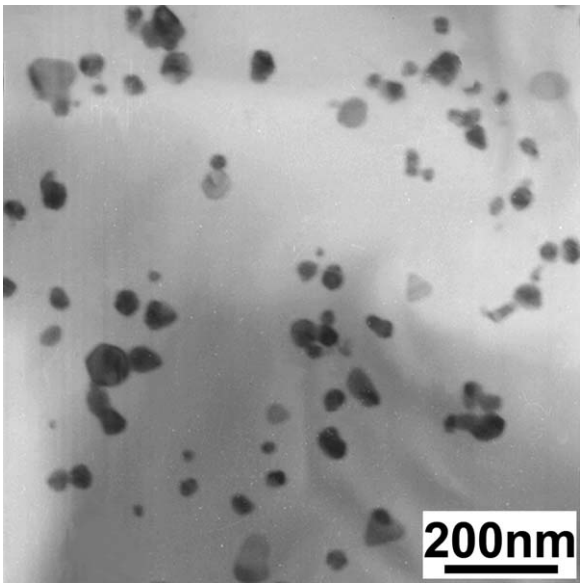

Figure 1. TEM micrograph of AgNPTs in the reduced PAH/PSS/PAH/PSS-Ag film.

H_2O_2 (aq.), $NaBH_4$, $AgNO_3$, and NaCl were all analytical reagents. Bacto-tryptone and yeast extract were from Fluka. Water used in all experiments had a resistivity higher than 18.2 MΩ cm.

Quartz and silicon slides were cleaned in a mixture of 70% H_2SO_4/30% H_2O_2 (caution: named as the piranha solution, a strong oxidizer and should not be stored in sealed containers) under ultrasonication at 80°C for 30 min, thoroughly rinsed with water and dried with pure N_2 stream.

Preparation of PSS-Ag Complex

Sixty milliliter 5 mg/mL PSS solution was added dropwise in 30 mL 18 mg/mL $AgNO_3$ solution under stirring. After complete complexation of PSS anions with Ag^+ cations for 1 h, the PSS-Ag complex solution was stored in a brown volumetric flask against decomposition by natural light.

Fabrication of Horizontally Oriented AgNPTs

PAH and PSS were alternatingly deposited on solid slides through the LbL self-assembly technique. Each deposition consisted of immersing the slides in 2 mg/mL PAH or PSS or PSS-Ag solution for 20 min, rinsing with water for 5 min. After deposition of the PAH/PSS/PAH/PSS-Ag films, Ag in the PSS-Ag were reduced to AgNPTs by 0.01*M* $NaBH_4$ solution for 15 min, followed by rinsing with water for 5 min.

Characterization

The multilayers on silicon slides were observed by an Hitachi S-4800 scanning electron microscope (SEM, Japan) at an operation voltage of 3 kV. Multilayers with AgNPTs for the SEM observation were not sputtered with any metals like Pt. Multilayers on 230-mesh copper grids covered with Formvar films were observed with a JEM-100CXII transmission electron microscope (TEM, Japan) under an accelerating voltage of 100 kV and a vacuum of 10^{-6} Torr. The multilayers on mica were also characterized using a Nanoscope IIIa multimode AFM (Digital Instruments, USA) at a scan rate of 0.5 Hz in tapping mode at room temperature. X-ray photoelectron spectroscopy (XPS) for LbL films on silicon substrates was performed on a PHI5300 (USA) with a resolution of 0.80 eV under a vacuum of 1.3×10^{-5} Pa.

Antibacterial Test

The *S. aureus* was used to test the antimicrobial activity of the multilayers containing AgNPTs. A broth solution made from 1.0 g bacto-tryptone, 0.5 g yeast extract, 1.0 g NaCl, and 80 mL H_2O was adjusted to pH 7.2–7.4 and then diluted to l00 mL. The 100 mL broth was autoclaved and then refrigerated. Dissolving an *S. aureus* lyophilized pellet into 25 mL of broth, *S. aureus* bacteria in broth were prepared, followed by incubation for 24 h at 37.0°C under shaking. Once cloudiness formed, the broth was refrigerated to keep bacteria at a dormant state until later tests. To reactivate the *S. aureus* bacteria, 25 mL refrigerated broth was incubated for 5 h at 37.0°C under shaking.

The antibacterial activity of films against S. aureus was studied by a film contact method. All the samples including the films and the NaCl powder were first sterilized by autoclave at 121.0°C for 40 min. The 100 μL 1×10^6 colony-forming unit (CFU)/mL *S. aureus* solutions were separately dropped on 20×25 mm^2 films with and without AgNPTs, the latter films were for control experiments. The films immersed in the bacterial solutions were sealed with aseptic polyethylene films and incubated at 37.0°C overnight. 10 mL 0.9% NaCl solutions were used separately to rinse the films thoroughly then diluted 5 times. Hundred microliter above diluted solutions were inoculated onto a standard agar culture medium and incubated at 37.0°C for 24 h. Then bacterial colonies were counted.

RESULTS AND DISCUSSION

Assembly of Horizontally Oriented AgNPTs in the Polyelectrolyte Matrix

TEM observation shows that Ag nanoparticles in the polyelectrolytes matrix appear as AgNPTs in various shapes including

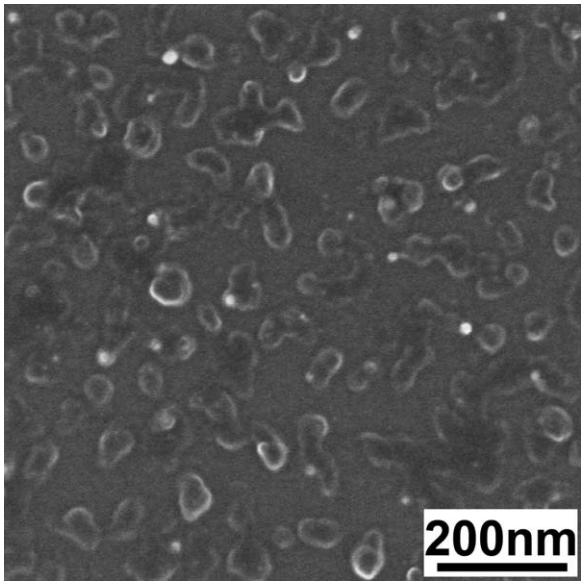

Figure 2. SEM micrograph of AgNPTs in the reduced PAH/PSS/PAH/PSS-Ag film.

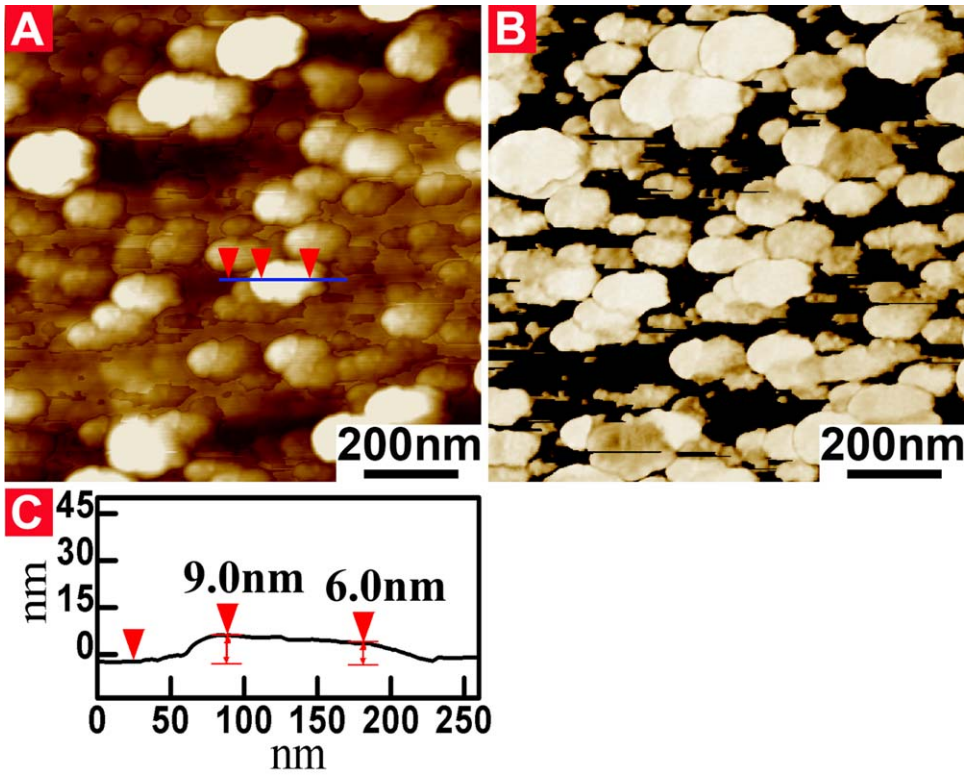

Figure 3. AFM (A) height and (B) phase images of AgNPTs in the reduced the PAH/PSS/PAH/PSS-Ag film, (C) Section analysis for the line in (A). [Color figure can be viewed in the online issue, which is available at wileyonlinelibrary.com.]

hexagonal, and truncated triangular, with the average lateral dimension of 20 nm (Figure 1). Such AgNPTs have been observed in solution synthesis processes,[22] rather than in two dimensional film systems as in this work. The AgNPTs spread across the whole films, orienting parallel to the film surface.

In the experiment Cu grids were covered with Formvar films, which separated the polyelectrolyte multilayers from the Cu grids. In addition, the Ag^+ cations in the PSS-Ag complexes in the multilayers are not freely movable with a large diffusion coefficient as those in solution. So the possibility that AgNPTs are formed via a displacement reaction between the Ag^+ cations and the Cu grids can be neglected.

Figure 2 shows the SEM micrograph of AgNPTs in the reduced PAH/PSS/PAH/PSS-Ag multilayers. The image contrast is not sharp enough, since the samples are not sputtered with gold or platinum to assure accurate results, avoiding crystallization of foreign metallic species. AgNPTs can be well distinguished, also averagely about 20–80 nm wide, consistent with the TEM results.

Figure 3 shows the AFM images and section analysis of the reduced PAH/PSS/PAH/PSS-Ag film. AgNPTs distribute homogeneously over the polymer matrix [Figure 3(A)], which can be better observed in the phase image [Figure 3(B)]. AgNPTs might be either totally above or partially buried in the underlying polymer layers. The PAH/PSS/PAH layers below the PSS-Ag outermost layer are about 3 nm. It is difficult to know that how deep the AgNPTs are buried. The AgNPTs above the polymer layers is about 9 nm thick, as obtained from the section analysis [Figure 3(C)]. The AgNPTs are thus estimated to have the thickness of 9–12 nm, nearly equal to that of the total multilayers. Consistent with the TEM and SEM results, the nanoplates spread across the whole film and all nearly orient horizontally to the film surface. Since the polyelectrolyte molecules in one layer interdigitate intimately with the neighboring stratified layer, one can not rule out the possibility that some AgNPTs are embedded with some tilted angle in the ultrathin film.

All the microscopic characterization results confirm the horizontally oriented AgNPTs obtained in the polyelectrolyte matrix. The size and density of AgNPTs shown by TEM, SEM, and AFM are different, which might be due to the slightly different depositing processes on specific substrates (Si slides for SEM, Cu grids covered with Formvar films for TEM and mica for AFM, respectively).

Figure 4 shows the XPS of reduced PAH/PSS/PAH/PSS-Ag films on silicon slides. Referring to the standard binding energy, characteristic peaks of Ag_{3d} (368.06, 374.21 eV), N_{1s} (400.60 eV), C_{1s} (284.60 eV), and O_{1s} (531.76 eV) can be clearly observed [Figure 4(A)]. The characteristic Ag3d peaks further confirm the existence of Ag in the polyelectrolyte matrix. The mass fraction of AgNPTs can not be simply provided by calculating the peak areas, since XPS can not provide accurate quantitative results of elemental components. In addition, hydrogen atoms could not be detected.

Because of the energy level split by the interaction between the orbital and the spin of electrons, the spectra of *p*, *d*, and *f*

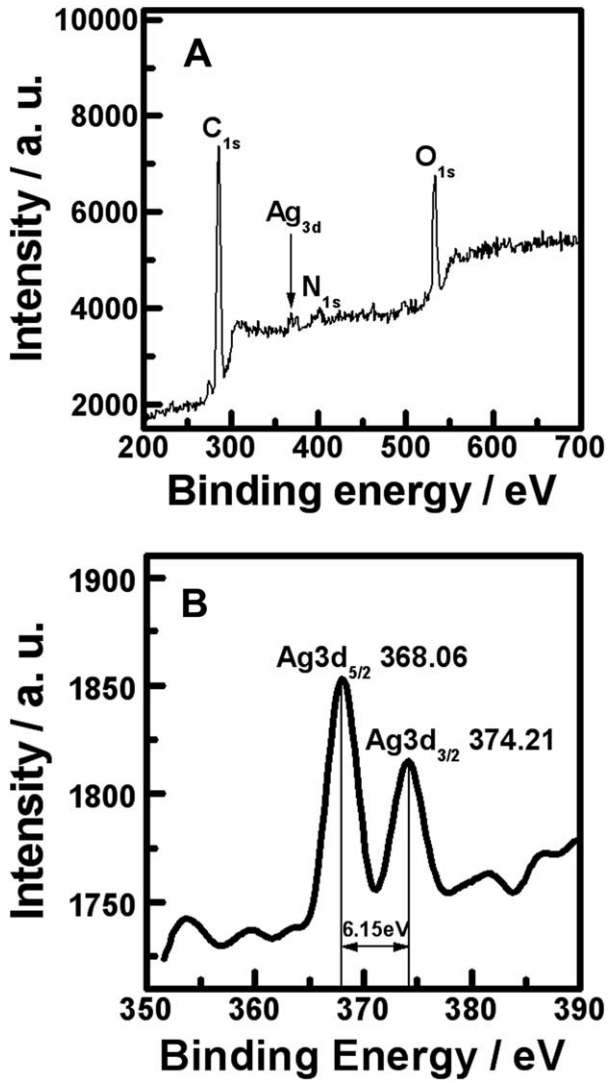

Figure 4. XPS of AgNPTs in the reduced PAH/PSS/PAH/PSS-Ag film. Peaks in the range of 350–390 nm in (A) are magnified in (B).

photoelectrons of Ag atoms show double lines. Figure 4(B) shows that the experimental energy spacing between the binding energy of $Ag_{3d5/2}$ (368.06 eV) and the $Ag_{3d3/2}$ (374.21 eV), $\Delta(E(Ag_{3d3/2}) - E(Ag_{3d5/2})^{experimental}$, is 6.15 eV. The theoretical energy spacing between them is normally consistent. In other words, the $\Delta(E(Ag_{3d3/2}) - E(Ag_{3d5/2}))^{experimental}$-$\Delta(E(Ag_{3d3/2}) - E(Ag_{3d5/2}))^{theoretical}$ should be less than 0.2 eV. The $\Delta(E(Ag_{3d5/2}) - E(Ag_{3d3/2}))^{theoretical}$ is 6.00 eV, 0.15 eV less than $\Delta(E(Ag_{3d5/2}) - E(Ag_{3d3/2})^{experimental}$, in good consistence with the expected difference, 0.20 eV. As a result, XPS patterns prove the existence of Ag atoms in the polymer films.

The Antibacterial Activity

The antibacterial activity of AgNPTs in polyelectrolyte multilayers was studied by a film contact method against *S. aureus*. The control experiment shows that many colonies of *S. aureus* distribute on nutrient agar medium [Figure 5(A)], after inoculation and incubation of *S. aureus* from their solutions treated by the PAH/PSS films without AgNPTs. On the contrary, no colonies of *S. aureus* exist on nutrient agar medium [Figure 5(B)], after inoculation and incubation of the same amount of *S. aureus* bacteria from their solutions treated by the reduced PAH/PSS/PAH/PSS-Ag films containing horizontally oriented AgNPTs. The reason should be that the AgNPTs kill the living *S. aureus* in the solution immersing the AgNPTs-films during the incubation at 37.0°C overnight, so no living *S. aureus* bacteria exist. After inoculation on the standard agar culture medium and incubation at 37.0°C for 24 h, the killed *S. aureus* can not proliferate, so no bacteria colonies can be observed. The assembled AgNPTs in polyelectrolytes matrix are thus proved to have excellent antimicrobial activity.

As the mostly used reductant in the past decades, $NaBH_4$ is chosen in our work to reduce the Ag in the PSS-Ag to Ag nanostructures. It is interesting that only horizontally oriented and homogeneously distributed AgNPTs form in the polyelectrolyte matrix. The aspect ratio (width, 20–80 nm; divided by thickness, 9–12 nm) of nanoplates is about 1.7–8.9. Other Ag nanostructures such as nanocubes, nanorods, or nanowires do not appear. It is worth discussing the formation mechanism of these well aligned AgNPTs.

On one hand, these AgNPTs forming in the films should be due to the characteristics of the LbL technique, which well aligns the PSS-Ag, PSS, and PAH molecules in a periodic layered structure. Such stratified structures with oppositively charged polyelectrolytes of individual layers interdigitating intimately have been well documented by Lösche and co-workers using neutron reflectometry.[23] During the deposition of the positively charged PAH on negatively charged solid slides (e.g., quartz or silicon), the PAH forms a planar layer. In the following deposition of negatively charged PSS on PAH, the PSS also forms a planar layer, so do other layers of PAH, PSS, and PSS-Ag. Regarding to the PSS-Ag layer, it confines the location of Ag^+ cations in a planar way. Reduced by $NaBH_4$, Ag^+ in PSS-Ag form Ag nanoparticles, which also distribute in a planar way. On the other hand, the horizontal orientation and homogeneous distribution of AgNPTs should be attributed to the diffusion of Ag nanoparticles confined by PSS and PAH. PSS-Ag has free $—SO_3^-$ groups, which can form complex with Ag^+. PSS-Ag also has the $—SO_3$-Ag groups, which are later reduced to $—SO_3H$ groups and Ag. Both the $—SO_3^-$ and $—SO_3H$ groups on the side chains of layered PSS decrease the diffusion speed of Ag atoms and Ag nanoparticles, favorable for the parallel diffusion direction of Ag

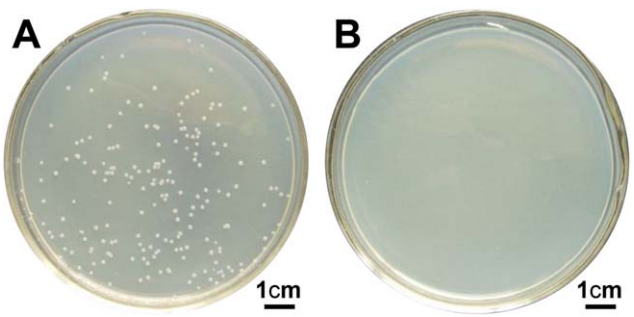

Figure 5. Antibacterial activity of (A) the PAH/PSS film as the control experiment and (B) the reduced PAH/PSS/PAH/PSS-Ag film. [Color figure can be viewed in the online issue, which is available at wileyonlinelibrary.com.]

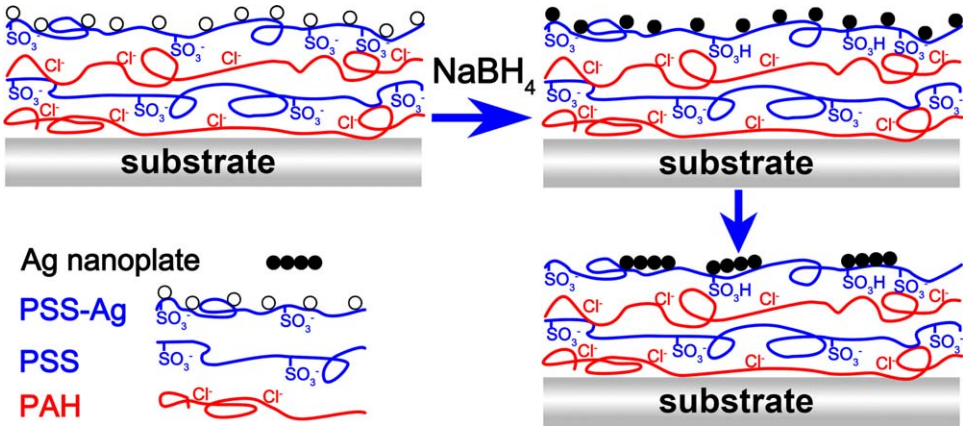

Figure 6. Schematic formation of horizontally oriented AgNPTs in the polyelectrolyte matrix of PAH, PSS and PSS-Ag under reduction by $NaBH_4$. In the uppermost layer of the PSS-Ag complex, the SO_3^- groups complexing the Ag cations are not all illustrated. [Color figure can be viewed in the online issue, which is available at wileyonlinelibrary.com.]

atoms and Ag nanoparticles to form layered nanoplates near the layered PSS. Figure 6 illustrates the schematic formation of AgNPTs in the polyelectrolyte matrix.

There are articles on hybrid polyelectrolyte-Ag films. However, they are either about direct assembly of Ag nanoparticles in the LbL films[24,25]; or on later immersion of the polyelectrolyte multilayers in a silver(I) solution precursor followed by different reduction methods.[26–28] By immersing the polyelectrolyte multilayers containing PAH/PAA (PAA denotes poly-acrylic acid) in a silver acetate aqueous solution, followed by reduction with H_2[26] (or dimethylamine borane, DMAB[27]), or ambient light (or UV light)[28], Ag nanoparticles without specific morphology forming in the films are documented. By our strategy with PSS-Ag as silver precursor, we observe the only horizontally oriented AgNPTs. Obviously, the final geometry and orientation of silver nanostructures depends on detailed assembly parameters. Whether it is possible to get other silver nanostructures with the present silver precursor will be focused in the next study by manipulating experimental parameters.

CONCLUSIONS

With a strategy of making good use of ordered packing of polyelectrolytes multilayers on planar substrates, we have assembled horizontally oriented AgNPTs by reduction of PSS-Ag. The AgNPTs with exposed crystal faces of low energy have active antibacterial activity. The interaction of reduced Ag atoms and Ag nanoparticles with the $-SO_3^-$ and the $-SO_3H$ groups in PSS confines the diffusion of Ag atoms and Ag nanoparticles, resulting in the formation of horizontally oriented AgNPTs. This work provides a new path to realize controlled orientation of metallic nanoplates. It also provides insight between the relationship of antimicrobial behavior and the specific nanostructure of silver. Concerning specific antibacterial activity of the horizontally oriented AgNPTs for the most economical use of silver, comparison by ongoing works between these AgNPTs to those vertically oriented ones or even smooth silver surface will highlight the strategy in this work.

ACKNOWLEDGMENTS

The authors thank the National Natural Science Foundation of China (21273135, 21403128), Independent Innovation Foundation of Shandong University (2011JC026) and Natural Science Foundation of Shandong Province (ZR2010BM039).

REFERENCES

1. Yi, Z.; Li, X.; Xu, X.; Luo, B.; Luo, J.; Wu, W.; Yi, Y.; Tang, Y. *Colloids Surf. A* **2011**, *392*, 131.
2. Tang, J.; Chen, Q.; Xu, L. G.; Zhang, S.; Feng, L. Z.; Cheng, L.; Xu, H.; Liu, Z.; Peng, R. *ACS Appl. Mater. Interfaces* **2013**, *5*, 3867.
3. Lu, Q.; Lee, K.-J.; Lee, K.-B.; Kim, H.-T.; Lee, J.; Myung, N. V.; Choa, Y.-H. *J. Colloid Interface Sci.* **2010**, *342*, 8.
4. Rahmansyah, N.; Lo, C.-T.; Syu, C.-M.; Lee, C.-L. *J. Appl. Polym. Sci.* **2011**, *122*, 1236.
5. Brandon, M. P.; Ledwith, D. M.; Kelly, J. M. *J. Colloid Interface Sci.* **2014**, *415*, 77.
6. Wang, D. H.; Kim, J. K.; Lim, G.-H.; Park, K. H.; Park, O. O.; Lim, B.; Park, J. H. *RSC Adv.* **2012**, *2*, 7268.
7. Lee, C.-L.; Yang, H.-L.; Chen, C.-W.; Tsai, Y.-L. *Electrochim. Acta* **2013**, *106*, 411.
8. Zhu, C.; Meng, G.; Huang, Q.; Zhang, Y.; Tang, H.; Qian, Y.; Chen, B.; Wang, X. *Chem. Eur. J.* **2013**, *19*, 9211.
9. Gao, M.; Sun, L.; Wang, Z.; Zhao, Y. *Mater. Sci. Eng. C* **2013**, *33*, 397.
10. Lin, J. J.; Lin, W. C.; Li, S. D.; Lin, C. Y.; Hsu, S. H. *ACS Appl. Mater. Interfaces* **2013**, *5*, 433.
11. Lukman, A. I.; Gong, B.; Marjo, C. E.; Roessner, U.; Harris, A. T. *J. Colloid Interface Sci.* **2011**, *353*, 433.
12. Huang, L. J.; Zhai, Y. M.; Dong, S. J.; Wang, J. *J. Colloid Interface Sci.* **2009**, *331*, 384.
13. Chen, D.; Zhu, X.; Zhu, G.; Qiao, X.; Chen, J. *J. Mater. Sci.: Mater. Electron.* **2012**, *23*, 625.
14. Zhang, Q.; Yang, Y.; Li, J.; Iurilli, R.; Xie, S.; Qin, D. *ACS Appl. Mater. Interfaces* **2013**, *5*, 6333.
15. An, J.; Tang, B.; Ning, X. H.; Zhou, J.; Xu, S. P.; Zhao, B.; Xu, W. Q.; Corredor, C.; Lombardi, J. R. *J. Phys. Chem. C* **2007**, *111*, 18055.
16. Sun, Y. G.; Qiao, R. *Nano Res.* **2008**, *1*, 292.

17. Liu, G. Q.; Cai, W. P.; Kong, L. C.; Duan, G. T.; Lu, F. J. *J. Mater. Chem.* **2010**, *20*, 767.
18. Decher, G. *Science* **1997**, *277*, 1232.
19. Min, N. B. Physical Theory on Crystal Growth; Shanghai Science and Technology Press: Shanghai, **1982**.
20. Brice, J. *J. Cryst. Growth* **1970**, *6*, 205.
21. Gilman, J. J. The Art and Science of Growing Crystals; Wiley: New York, **1963**.
22. Jana, D.; Mandal, A.; De, G. *ACS Appl. Mater. Interfaces* **2012**, *4*, 3330.
23. Lösche, M.; Schmitt, J.; Decher, G.; Bouwman, W. G.; Kjaer, K. *Macromolecules* **1998**, *31*, 8893.
24. Sripriya, J.; Anandhakumar, S.; Achiraman, S.; Antony, J. J.; Siva, D.; Raichur, A. M. *Int. J. Pharm.* **2013**, *457*, 206.
25. Soltwedel, O.; Ivanova, O.; Hohne, M.; Gopinadhan, M.; Helm, C. A. *Langmuir* **2010**, *26*, 15219.
26. Wang, T. C.; Rubner, M. F.; Cohen, R. E. *Langmuir* **2002**, *18*, 3370.
27. Lee, D.; Cohen, R. E.; Rubner, M. F. *Langmuir* **2005**, *21*, 9651.
28. Machado, G.; Beppu, M. M.; Feil, A. F.; Figueroa, C. A.; Correia, R. R. B.; Teixeira, S. R. *J. Phys. Chem. C* **2009**, *113*, 19005.